

Mechanosensation and mechanical load modulate the locomotory gait of swimming *C. elegans*

Jeremie Korta¹, Damon A. Clark¹, Christopher V. Gabel¹, L. Mahadevan^{2,3} and Aravinthan D. T. Samuel^{1,*}

¹Department of Physics, ²Division of Engineering and Applied Sciences and ³Department of Organismic and Evolutionary Biology, Harvard University, Cambridge, MA 02138, USA

*Author for correspondence (e-mail: samuel@physics.harvard.edu)

Accepted 25 April 2007

Summary

Animals move through their environments by selecting gaits that are adapted to the physical nature of their surroundings. The nematode *Caenorhabditis elegans* swims through fluids or crawls on surfaces by propagating flexural waves along its slender body and offers a unique opportunity for detailed analysis of locomotory gait at multiple levels including kinematics, biomechanics and the molecular and physiological operation of sensory and motor systems. Here, we study the swimming gait of *C. elegans* in viscous fluids in the range 0.05–50 Pa s. We find that the spatial form of the swimming gait does not vary across this range of viscosities and that the temporal frequency of the swimming gait only decreases by about 20% with every 10-fold increase in viscosity. Thus, *C. elegans* swims in low gear, such that its musculature can deliver mechanical force and power nearly 1000-fold

higher than it delivers when swimming in water. We find that mutations that disrupt mechanosensation, or the laser killing of specific touch receptor neurons, increase the temporal frequency of the undulating gait, revealing a novel effect of mechanosensory input in regulating the putative central pattern generator that produces locomotion. The adaptability of locomotory gait in *C. elegans* may be encoded in sensory and motor systems that allow the worm to respond to its own movement in different physical surroundings.

Supplementary material available online at
<http://jeb.biologists.org/cgi/content/full/210/13/2361/DC1>

Key words: nematode, locomotion, mechanosensation, *Caenorhabditis elegans*.

Introduction

Undulating propulsion is utilized by a wide variety of swimming and gliding animals, including worms, leeches and slender fish, and has been extensively analyzed at the level of external kinematics and at the level of internal sensorimotor control. For small, slender organisms moving in a viscously dominated environment, resistive-force theory enabled Gray and Hancock to quantify the forces and torques along the bodies of elongate swimmers and to calculate propulsive speed as a function of the spatiotemporal dynamics of the locomotory gait (Gray and Hancock, 1955). While much of this work was motivated by and applied to the movements of microscopic swimmers such as spermatozoa and bacteria, it is just as applicable to larger swimmers moving in a hydrodynamic environment where inertia is dominated by viscous forces, i.e. where the Reynolds number is less than unity. However, the connection between external kinematics and the internal sensorimotor circuits that govern the adaptability of gait in different environments remains largely unexplored.

The nematode *Caenorhabditis elegans* provides a model system that allows rigorous analyses of locomotory gait at

multiple levels. One advantage is anatomical simplicity. The *C. elegans* nervous system contains precisely 302 neurons with a stereotyped wiring diagram, and undulating propulsion is driven by rhythmic activity of 95 muscle cells that line its dorsal and ventral sides (White et al., 1976; White et al., 1986). Another advantage is straightforward hydrodynamics, as the Reynolds numbers of swimming *C. elegans* are less than unity (Purcell, 1977). Finally, *C. elegans* offers genetic accessibility, facilitating an analysis of locomotory gait that traverses the levels of genetics, neurophysiology and behavior.

Most studies of *C. elegans* behavior involve crawling motility on agar surfaces. *C. elegans* improves its own crawling efficiency on soft agar surfaces by incising a sinusoidal groove, thereby reducing lateral slipping of its body against the groove. Moreover, crawling worms use undulations with shorter wavelength and slower temporal frequency than swimming worms. These differences underscore the adaptability of locomotory gait in response to the physical nature of the external medium. However, crawling locomotion is particularly complicated when analyzing external kinematics: in principle, one has to take into account the surface tension

that holds the worm to the agar surface, the forces that incise the groove, the variable friction and tension along the length and around the perimeter of the worm's cylindrical body, and so on. Thus, Gray and Lissman focused on swimming locomotion in their classic analysis relating the speed of progression of nematodes to the form and frequency of their undulating waves (Gray and Lissman, 1964).

Using *C. elegans*, it may be possible to connect the adaptability of locomotory gait to the genetics and physiological operation of sensory and motor systems. In a recent analysis, Karbowski et al. showed that the spatial form and temporal frequency of the crawling gait is largely independent of external physical parameters, including worm size and the rigidity of the agar surface, and that the crawling gait is unaffected by many mutations that affect neurons and muscle (Karbowski et al., 2006). At the molecular level, Tavernarakis et al. showed that mutation of the *mec-6* or *unc-8* genes, which encode subunits of mechanically gated ion channels, leads to an irregular crawling gait with reduced amplitude and wavelength (Tavernarakis et al., 1997), suggesting that mechanosensory systems may play an important role in locomotory gait. Li et al. discovered that mutation of the *trp-4* gene, which encodes a mechanosensitive TRPN channel expressed in the DVA interneuron, leads to a crawling gait with increased amplitude and speed (Li et al., 2006), thus identifying a molecular and neuronal pathway for proprioception in regulating the crawling gait.

Here, we focus on the adaptability of locomotory gait for the more tractable case of swimming *C. elegans*. The movement of slender objects through viscous fluids at low Reynolds numbers is well understood, allowing us, like Gray and Lissmann (Gray and Lissmann, 1964), to precisely calculate the flow field surrounding the swimming worm, the normal and transverse forces at each point on the worm's surface and thus the speed and efficiency of undulating propulsion. By analyzing the movements of individual worms swimming in fluids containing different amounts of the viscous agent methylcellulose, we characterize the effects of increasing mechanical load on the forward swimming gait. We also characterize the contribution of mechanosensory feedback to the swimming gait by quantifying the effects of mechanosensory mutation and laser ablation of touch receptor neurons. Our observations lay groundwork for analyzing the effects of mechanical load and mechanosensory input in the adaptability of locomotory gait for swimming *C. elegans*.

Materials and methods

Strains

Caenorhabditis elegans wild-type Bristol N2 were cultivated at 20°C using standard methods (Brenner, 1974). The *mec-4(d)* mutant strain was obtained from Monica Driscoll (Rutgers, Piscataway, NJ, USA) and the *mec-6(u450)* mutant strain was obtained from the *C. elegans* Genetics Center (Minneapolis, MN, USA).

Laser ablation

We followed techniques established for standard laser microsurgery (Bargmann and Avery, 1995), except that we used an ultrafast Ti:sapphire laser to generate the laser pulses (Chung et al., 2006). To facilitate the identification and killing of ALM and PLM neurons in L1 worms, we used transgenic worms that expressed the *mec-4::gfp* transgene in those neurons. Each larval animal was anesthetized with 0.2–0.8 mmol l⁻¹ sodium azide and mounted on a thin pad of 2% agarose. Using fluorescence microscopy, each neuronal target was moved to the focal point of laser pulses and ablated. After surgery, worms were recovered within 30 min by placing them on fresh plates with bacterial food. After recovery, worms were returned to overnight incubation before undergoing behavioral assays as young adults.

Methylcellulose

Stock solutions of viscous fluid were prepared by adding certain amounts of methylcellulose (Sigma, St Louis, MO, USA) to NGM buffer (Sulston and Hodgkin, 1988) and stirring overnight at 4°C. We determined the viscosity of each solution by quantifying the sedimentation rate of small beads dropped into each fluid. Methylcellulose is a polymeric material that behaves like a viscoelastic liquid at high strain rates but exhibits Newtonian hydrodynamics at sufficiently low shear rates. The typical shear rates exhibited by swimming *C. elegans* in our experiments were ~15 s⁻¹. In order to show that non-Newtonian effects were negligible for the shear rates exhibited by swimming *C. elegans* in our experiments, we used sedimentation experiments to verify the transverse and longitudinal frictional drag coefficients of thin metal rods with similar size and aspect ratio of adult *C. elegans*.

Video analysis

Individual young adult worms were removed from overnight cultivation at 20°C, rinsed in NGM buffer and immersed in a viscous solution made with NGM buffer and defined concentrations of methylcellulose. The worm was obliquely illuminated to render the worm's body in sharp contrast to a dark background. A CCD camera equipped with a zoom lens was used to capture images of the swimming worms at 30 Hz, and 10 s movie clips were recorded using LabVIEW (National Instruments, Austin, TX, USA).

We used our own machine-vision algorithms written in Matlab (MathWorks, Inc., Natick, MA, USA) to analyze those movie clips in which the worm was observed to be swimming within the focal plane and within the bulk liquid. We restricted our analysis to experiments in which the 0.1 mm-diameter worm was at least 5 mm away from the top and bottom surfaces of the liquid, where hydrodynamic corrections due to viscous coupling with the fluid surfaces would be <2% (Brenner, 1961). An edge-detection algorithm identified the *x*-*y* coordinates of all points along the dorsal and ventral sides of the swimming worm. The dorsal and ventral edges were least-squares fit with a Bezier spline (degree 5, 12 control points, open uniform knot),

rendering them continuous and differentiable (Cohen et al., 2001). Centerline points were calculated at the bisection of the vector connecting each point on the dorsal side to the nearest point on the ventral side. These midline points were then also fit to a Bezier spline and the coordinates of the body centerline were calculated at $N=100$ evenly spaced points from nose to tail (see Movie in supplementary material). The result was a continuous and smoothly differentiable mathematical description of the coordinates of the body centerline at each point in time – $[x_i(t), y_i(t)]$ from $i=1$ to N – simplifying subsequent numerical analysis of gait dynamics.

We used the coordinates of the body centerline to calculate the curvature as a function of body coordinate and of time, as well as the instantaneous velocity of each point along the body centerline. We calculated the curvature at each point along the body centerline within each video frame using the $N-1$ tangent angles along the centerline: $\theta_i = \arctan[(y_i - y_{i-1}) / (x_i - x_{i-1})]$. We calculated the velocity at each point along the body centerline using the coordinates from successive video frames: $\mathbf{u}_i = [x_i(t + \Delta t) - x_i(t), y_i(t + \Delta t) - y_i(t)] / \Delta t$.

These calculated velocities were used to determine the longitudinal and normal forces along the body centerline and swimming power using standard methods of resistive-force theory (Gray and Hancock, 1955).

Results

Video analysis of the swimming gait

We quantified the swimming gait of individual worms using video microscopy and machine-vision algorithms that analyze the posture of each worm in each video frame acquired at video rate. Cronin et al. developed a video-processing system for analyzing worm posture that automatically tracks the movements of discrete points distributed along the body centerline (Cronin et al., 2005). We developed a similar algorithm that tracks every point along the worm centerline afforded by video resolution and renders the worm centerline as a continuous, differentiable two-dimensional space curve. The instantaneous shape of the worm may be fully described by defining the curvature (the inverse of the radius of curvature) at each point along the worm's body (Fig. 1A) (see Movie in supplementary material). We define a body coordinate (l) along the body centerline along the total length from head ($l=0$) to tail ($l=L$). In terms of the tangential angle to each point along the centerline (ϕ) and the body coordinate, the curvature (κ) at each point is defined by:

$$\kappa = d\phi / dl. \quad (1)$$

Thus, the full spatiotemporal dynamics of the swimming gait may be represented in a contour plot that represents the time-varying curvature defined at points along the body centerline, $\kappa(l, t)$ (Fig. 1B).

In the contour plot, the undulating wave that drives forward-swimming may be traced by following regions of curvature traveling down the body coordinate. Since the body centerline is inextensible (length changes are $<5\%$ by our measurements),

the spatial and temporal dynamics of the swimming gait may be characterized using the undulation wavelength, number of waves and frequency. The undulation frequency is a well-defined metric that is straightforwardly measured by slicing along the time axis of the contour plot (Fig. 1B). However, defining and measuring the undulation wavelength is more complicated since the undulation of swimming worms is not perfectly sinusoidal and the number of wavelengths along the body centerline is nearly one. Wave speed, on the other hand, is a well-defined metric that may be straightforwardly measured by following the propagation of curvature along the body coordinate. Thus, a well-defined wavelength may be extracted from wave speed and undulation frequency using the equation, speed (m s^{-1}) = wavelength (m) \times frequency (Hz) (Fig. 1B).

In order to characterize the energetics and efficiency of the swimming gait, we require the time-varying hydrodynamic force against each segment of the worm's body within each undulation cycle. *C. elegans* is a microscopic, elongate swimmer about 1 mm in length (L) and 0.1 mm in diameter (d), allowing us to combine fluid dynamics at low Reynolds numbers and slender-body approximations in making these calculations. In the domain of low Reynolds number hydrodynamics, force is linearly proportional to velocity. Using video analysis, it is straightforward to quantify the instantaneous velocity of each point along the body centerline (Fig. 1C). To characterize the normal and tangential hydrodynamic force along the body centerline, we only need to multiply these velocities by frictional drag coefficients, C_N and C_L , associated with normal and longitudinal movements of slender objects (Berg, 1993). For example, for a prolate ellipsoid with length L and diameter d , these frictional drag coefficients in a fluid with viscosity η are:

$$C_L = \frac{2\pi\eta L}{\ln\left(\frac{2L}{d}\right) - \frac{1}{2}} \quad \text{and} \quad C_N = \frac{4\pi\eta L}{\ln\left(\frac{2L}{d}\right) + \frac{1}{2}}. \quad (2)$$

Mechanical load reduces the frequency but does not change the geometric shape of the swimming gait

Next, we quantified the effect of mechanical load on the shape and temporal dynamics of the swimming gait. We immersed individual young adult worms in solutions containing different amounts of the viscous agent methylcellulose, ranging from 0.5% methylcellulose at 0.05 Pa s to 3% methylcellulose at 50 Pa s (Berg and Turner, 1979), and monitored their forward-swimming movements using video microscopy. We found that the shape of the swimming gait characterized by its undulation wavelength is remarkably invariant across this 1000-fold increase in external mechanical load (Fig. 2A). However, we found that the undulation frequency exhibits a shallow dependence on mechanical load, dropping from about 2 Hz at 0.05 Pa s to 0.5 Hz at 50 Pa s (Fig. 2B).

Since the force required to move an object at low Reynolds numbers scales linearly with viscosity and speed, and the latter does not decrease very much as the viscosity is increased by

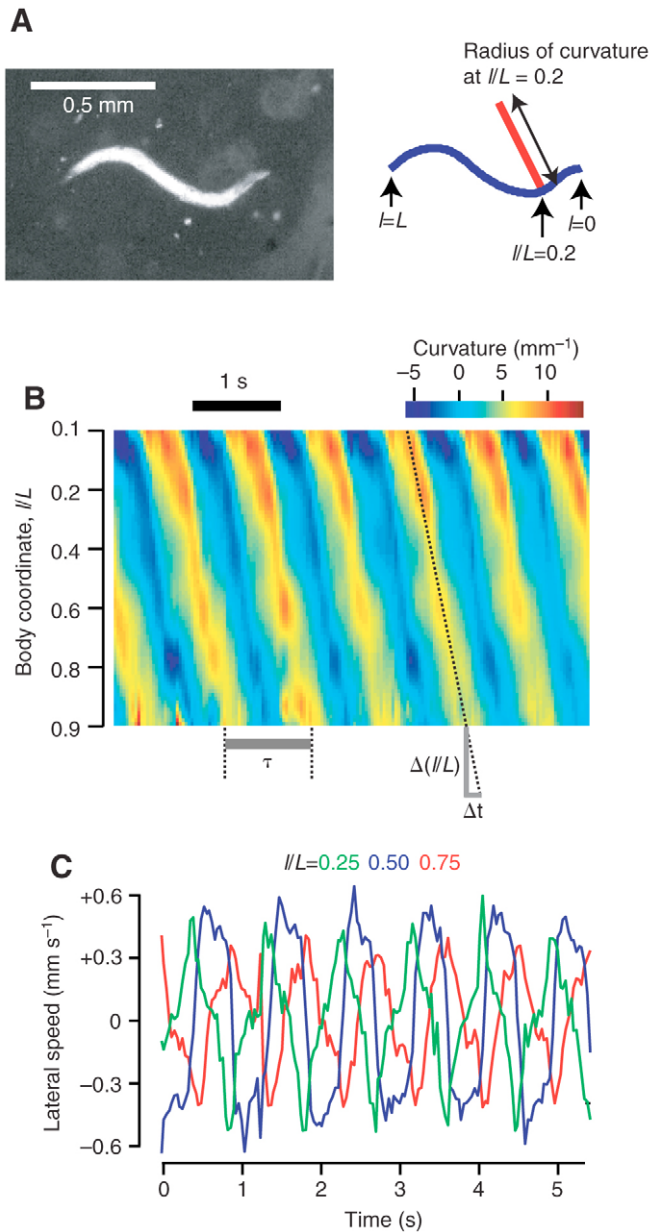


Fig. 1. The spatiotemporal dynamics of the swimming gait of *C. elegans*. (A) Dark-field video image of a young adult worm swimming in viscous fluid (0.5% w/w methylcellulose in NGM buffer) with its undulations within the focal plane of the microscope (also see Movie in supplementary material). Throughout this study, we used young adult worms of this size. In each video frame, custom-written machine-vision software fits a curve to the body centerline (blue line) and calculates the radius of curvature at each point along the body centerline (red line). We define a body coordinate that varies from $l=0$ at the head to $l=L$ at the tail. (B) Contour plot of the spatiotemporal dynamics of about six cycles of the forward-swimming gait represented as the curvature measured at each point along the body centerline over time. Values of curvature are scaled by color, with positive (negative) curvature indicating bend in the ventral (dorsal) direction. We show the body coordinate as the fractional distance along the body length (l/L) and display data corresponding to 0.1–0.9 to avoid showing the hyperflexible movements of the worm nose and whiplike tail. We measure temporal frequency by quantifying the time period (τ) between undulations. We measure the wave speed by quantifying the propagation of curvature down the body centerline. (C) To characterize the force and energetics of the swimming gait, we directly measured the velocity of each point along the body centerline throughout each undulation cycle. Here, we show the measurements of lateral speed, the direction orthogonal to the body centerline, at three different points along the body centerline through about six cycles of the forward-swimming gait. Positive (negative) speed indicates movement towards the ventral (dorsal) direction.

Removing mechanosensory input increases the frequency of the swimming gait

Effects of mechanical load on the swimming gait may appear at multiple levels, from mechanosensory input to the contractile mechanisms of muscle cells (Duysens et al., 2000). Mechanical load (the external hydrodynamic force on the swimming worm) and mechanosensation (the worm's ability to detect external forces) must be coupled at the level of external kinematics. In *C. elegans*, the genes and neurons that mediate mechanosensation have been extensively analyzed, providing us with an opportunity to dissect the specific contribution of mechanosensory input to the regulation of the swimming gait (Goodman and Schwarz, 2003). When the worm is gently touched on the head (tail), it responds by crawling backward (forward). The worm has six touch receptor neurons, also called microtubule cells, that mediate these touch responses. By laser ablating the touch receptor neurons, Chalfie et al. showed that either the ALML or ALMR neuron (the left and right anterior lateral microtubule cells) is required for the full response to touch on the head, that either the PLML or PLMR neuron (the left and right posterior lateral microtubule cells) is required for the full response to touch on the tail, that the AVM neuron (the anterior ventral microtubule cell) has only a weak contribution to touch responses to the head, and that the PVM neuron (the posterior ventral microtubule cell) does not contribute to touch responses (Chalfie et al., 1985).

Touch sensation by all of the touch receptor neurons may be altered by mutations in the *mec-4* and *mec-6* genes, which encode membrane proteins within the mechanosensory ion

many orders of magnitude, it follows that *C. elegans* is not force-limited as it swims in these very viscous fluids (Fig. 2C). The power dissipated in viscous shear (\bar{P}), a lower limit on the total power that the worm uses to swim, was obtained by integrating the products of force and velocity along the body centerline and averaging over an undulation cycle:

$$\bar{P} = \frac{1}{\tau} \int_0^{\tau} \int_0^L [C_L u_L(l,t)^2 + C_N u_N(l,t)^2] dl dt, \quad (3)$$

where τ is the undulation period, u_L and u_N are the longitudinal and normal velocities, respectively, l is length along the body and t is time. The dependence of the viscous power dissipation rate and viscosity (over the range of the viscosity where we were able to examine swimming worms) shown in Fig. 2C suggests that, in this regime, the worm is not power-limited either.

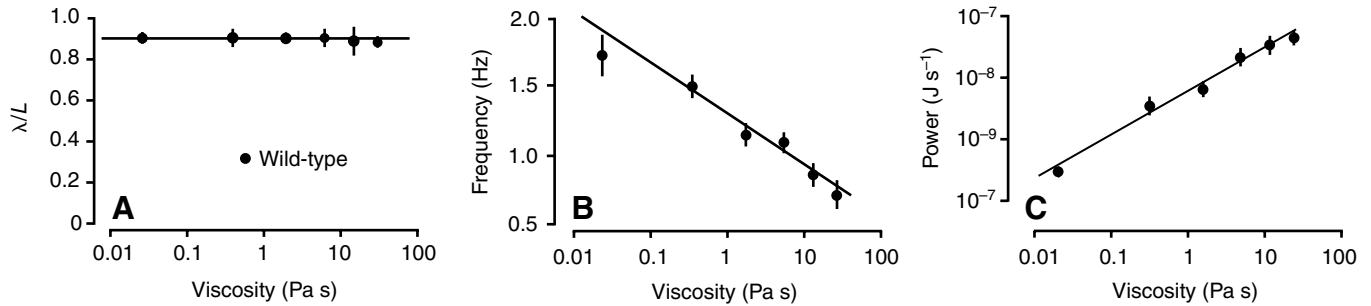


Fig. 2. Mechanical load affects the frequency but not the shape of the swimming gait. (A) The wavelength of the undulating gait of swimming worms does not vary with mechanical load. Here, we quantify the wavelength λ as a fraction of the total length of the body centerline. (B) The temporal frequency of the undulating gait of swimming worms drops with increasing mechanical load. (C) The mean power of the swimming gait calculated using Eqn 1 increases with swimming gait. The sublinear dependence (0.7 slope in a log–log plot) may be attributed to the drop in the temporal frequency of the swimming gait. Each measurement corresponds to data from 10–15 worms and 30–60 s of video (means \pm 1 s.e.m.). Solid lines represent linear regression fits.

channel complex (Chelur et al., 2002; O’Hagan et al., 2005). The *mec-4(d)* mutation leads to actual degeneration of the touch cells, thereby abolishing the touch response (Driscoll and Chalfie, 1991). The *mec-6(u450)* mutation interferes with the operation of mechanosensitive ion channels within the touch cells and also abolishes the touch response (Chelur et al., 2002). We examined both *mec-4(d)* and *mec-6(u450)* mutants in viscous fluids and found that neither mutation affects the shape of the swimming gait; both mutants exhibit the same undulation wavelength as wild-type worms in viscous fluids ranging from 0.05–50 Pa s (Fig. 3A). However, both mutations significantly affect the undulation frequency (Fig. 3B). Surprisingly, both *mec-4(d)* and *mec-6(u450)* mutant worms exhibit higher undulation frequencies than wild-type worms at each value of mechanical load. However, increasing mechanical load systematically reduces the undulation frequency of *mec-4(d)* and *mec-6(u450)* worms at nearly the same rate as wild-type worms.

We sought additional evidence that the touch receptor neurons are involved in regulating the swimming gait through laser ablation analysis. We used transgenic animals that expressed the *mec-4::gfp* transgene in a wild-type background, allowing us to target and laser ablate the ALM and PLM touch receptor neurons in larval animals. We found that ablating the ALM touch neurons has no effect on the shape of the swimming gait (Fig. 3C) but has the same effect on the undulation frequency as either the *mec-4(d)* or *mec-6(u450)* mutations (Fig. 3D). Ablating the PLM neurons has no effect on the shape of the swimming gait (Fig. 3C) and a lesser effect on the undulation frequency (Fig. 3D). Ablating both the ALM and PLM neurons was indistinguishable from killing ALM alone. These observations agree with the mutant analysis and suggest that much of the mechanosensory input that regulates the forward-swimming gait derives from the activity of the ALM touch receptor neurons.

Discussion

Understanding the mechanisms that allow an animal to adapt its locomotory gait to variable environments is a complex, multi-scale problem. Neuromuscular circuits within the animal

may regulate the time-varying spatial form and temporal frequency of locomotory gait by controlling patterns of activity in the body musculature. However, to allow for adaptive locomotory gait, these neuromuscular circuits must also adjust to the mechanics of the animal’s surroundings and actively respond to sensory feedback that is driven by the locomotory gait itself. Here, we have studied swimming *C. elegans* with the aim of establishing a tractable model to understand the interplay between external kinematics and internal sensorimotor dynamics in the adaptability of locomotory gait. We have shown that the swimming gait is remarkably robust. Increasing mechanical load by a factor of 1000 does not detectably affect the shape of the swimming gait and only slows its temporal frequency by a factor of 4. We have also shown that mechanosensory input through the touch receptor neurons, presumably activated by the self-movement of the worm experiencing the viscous resistance of the ambient fluid, has a direct effect on the temporal frequency of forward-swimming. This result bears comparison to the discovery by Li et al. that proprioceptive input that is mediated by the TRP-4 channel and the DVA interneuron affects the temporal frequency of the crawling gait (Li et al., 2006). Here, we discuss several implications of our results on the neuromuscular mechanisms and biomechanics that underlie the worm’s swimming gait.

The neuromuscular circuit in *C. elegans* that generates and maintains its rhythmic pattern of locomotory gait is not yet understood (Syntichaki and Tavernakis, 2004). In a central pattern generator (CPG) model proposed by Niebur and Erdos (Niebur and Erdos, 1993), a circuit in the nerve ring composed of command interneurons (AVA, AVB, AVD, and PVC) maintains rhythmic activity through synaptic interconnections within the circuit. This CPG then drives undulations through synaptic connections along the ventral nerve cord between the command interneurons and the motor neurons. Interestingly, these command interneurons are postsynaptic to the touch receptor neurons and are directly involved in the touch response. Chalfie et al., using systematic laser ablation analysis, showed that the ALM touch receptor neurons mediate most of the touch response to the head by stimulating AVB and

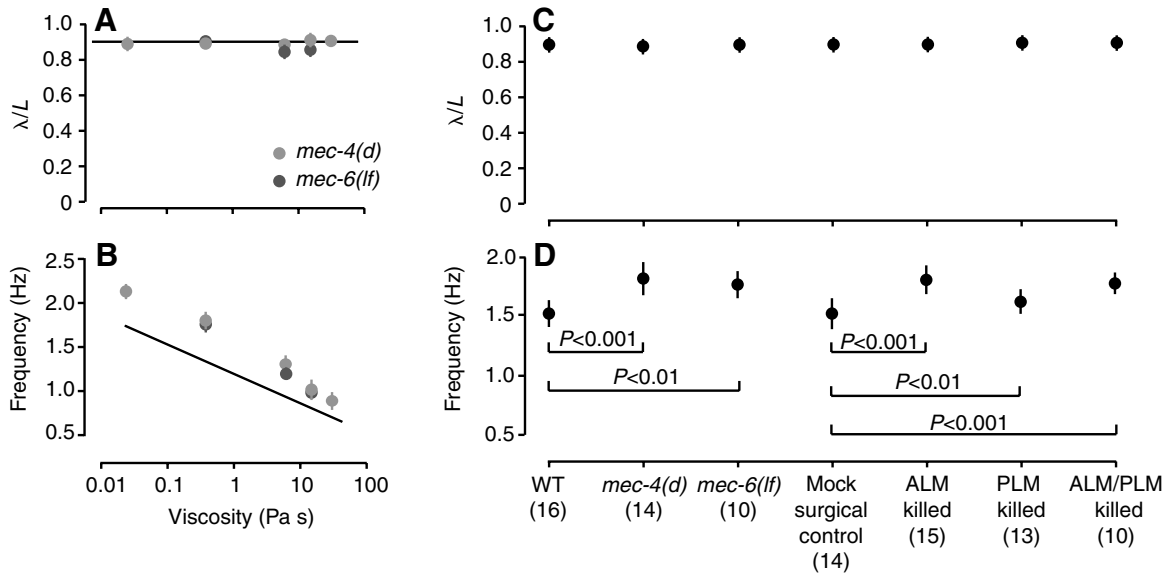


Fig. 3. Mechanosensory neurons affect the frequency but not the shape of the forward-swimming gait. (A) The shape of the forward swimming gait of *mec-4(d)* (light gray) and *mec-6(u450)* (dark gray) mutant worms does not vary with mechanical load. The solid line shows the line fit to wild-type data from Fig. 2A. (B) The temporal frequency of the swimming gait of *mec-4(d)* and *mec-6(u450)* mutants decreases with increasing mechanical load but is offset to higher temporal frequencies than in wild-type worms. The solid line shows the line fit to wild-type data from Fig. 2B. Each measurement in A and B corresponds to data from 10–15 worms and 30–60 s of video (means \pm 1 s.e.m.). (C) The shape of the forward-swimming gait of young adult worms in 1% methylcellulose is unaffected by the *mec-4(d)* or *mec-6(u450)* mutations or by ablation of the ALM or PLM touch receptor neurons. The number of worms analyzed in each measurement is shown in parentheses. Standard deviation errors bars, typically \pm 5% of the mean value of each measurement, are smaller than the data points. Neither *mec-4(d)* or *mec-6(u450)* mutants are distinguishable from wild-type ($P > 0.01$). None of the laser-ablated worms are distinguishable from the mock surgical controls, in which worms were prepared for laser surgery but not irradiated ($P > 0.01$). (D) The temporal frequency of the swimming gait of young adult worms is significantly increased by mutation or laser ablation. Error bars indicate one standard deviation. Differences between mutant and wild-type and between laser-ablated worms and mock surgical controls are indicated at $P < 0.01$ and at $P < 0.001$.

PVC, which trigger reverse movement, and inhibiting AVA and AVD, which trigger forward movement (Chalfie et al., 1985). They also showed that the PLM touch receptor neurons mediate the touch response to the tail by having precisely opposite effects on the command interneurons (Chalfie et al., 1985). One possibility is that the touch receptor neurons, in addition to mediating the reflexive touch responses, also affect the frequency of the swimming gait by altering the temporal dynamics of the CPG, a direct consequence of their rhythmic activation by the external forces caused by movement. Thus, removing the ALM neurons, which trigger reverse movement and conceivably have an antagonistic effect on forward movement, might increase the temporal frequency of the swimming gait. However, it is unclear why removing the PLM neurons, which presumably have an opposite relationship with the command interneurons, also increases the speed of forward movement, albeit by a lesser amount. These surprising observations may be clarified by better dynamical models of the CPG circuits that incorporate the effects of mechanosensory input and the worm's self-movement in its surroundings.

Our observations support basic conclusions about the biomechanics of self-propulsion in *C. elegans*. One possibility is that the forces required to displace the surrounding fluid as the worm swims are negligible in comparison to the forces required to bend its rigid body. In any case, *C. elegans* is

capable of generating much higher propulsive forces under mechanical load than in water. In other words, *C. elegans* effectively swims in low gear, which might have direct ecological relevance, enabling the animal to burrow through soil, a natural habitat where it likely encounters higher mechanical loads than when swimming in water. Another striking observation is that the shape of the swimming gait is invariant over 1000-fold changes in mechanical load. When swimming, the worm has only about one wavelength of undulation along its body, whereas when crawling it has closer to two (Karbowski et al., 2006). One possibility is that the variation in the shape of the locomotory gait is a simple function of mechanical load. We originally thought that swimming in water might represent the low end of mechanical load (characterized by a swimming gait with large wavelength and high temporal frequency) and crawling on agar surfaces might represent the high end of mechanical load (characterized by small wavelength and low temporal frequency), and that by progressively varying mechanical load through viscosity we might uncover a gradual transformation in the spatiotemporal dynamics of gait with intervening wavelengths and frequencies. Gait may still be a straightforward function of mechanical load: the mechanical load of the most viscous aqueous solution that we were able to make with methylcellulose (\sim 50 Pa s at 3% w/w) is probably lower than

that required to crawl on agar surfaces, and the transition between the swimming and crawling gaits may be more subtle. For example, eelworm larvae exhibit a transition from a crawling to swimming gait that may be evoked by gradually increasing the film thickness of water on a substrate on which the eelworm larvae crawl (Wallace, 1959).

It may be possible, however, that the swimming and crawling gaits are well-adapted solutions to fundamental differences in the mechanics of swimming at low Reynolds numbers and crawling on agar surfaces. When crawling, *C. elegans* incises ridges into the agar surface with its body, pushing laterally and sliding longitudinally along these ridges. This strategy improves crawling efficiency by making the frictional drag coefficient for normal movement (C_N) much higher than the frictional drag coefficient for longitudinal movement (C_L). However, when swimming at low Reynolds number in Newtonian fluids, the 1:2 ratio between C_N and C_L is fixed. Gray and Hancock showed that the calculated speed of a slender object propelling itself by undulating waves at low Reynolds numbers depends on the relative values of C_N and C_L , which are prescribed by hydrodynamics (Gray and Hancock, 1955). Holwill and Burge (Holwill and Burge, 1963) extended the analysis of such swimmers to include considerations of energetics and efficiency. They found that the hydrodynamic efficiency – defined as the ratio between the power that the undulatory swimmer would use to move at a particular speed and the power that an external agent would use to pull the swimmer passively at the same speed, a quantity that is independent of the viscosity of the fluid for low Reynolds number movements – reaches a peak when the swimmer uses one undulation wavelength over its entire body. Thus, *C. elegans*, although it can change the shape of its locomotory gait, may opt to use the same spatial form in various Newtonian fluids in order to maximize hydrodynamic efficiency. In order to explore the transformation of gait in different environments, it may be useful to study the movements of *C. elegans* in environments where the ratio between C_L and C_N may be varied systematically.

C. elegans provides a rare opportunity to analyze locomotory gait that connects our understanding of the genetics and neurobiology of mechanosensory transduction (Goodman and Schwarz, 2003) at the molecular level with the mechanics of low-Reynolds number hydrodynamics at the organismal level (Purcell, 1977). Here, we have taken advantage of these tools to isolate and quantify specific effects of mechanosensory and mechanical load on the swimming gait. Our analysis highlights new questions: *C. elegans* opts to use the same spatial form when swimming in fluids with different viscosity, but does it do so because only certain spatial forms of locomotory gait are hardwired into its motor systems or because the worm is using biochemical feedback to maximize hydrodynamic efficiency? Mechanosensory input affects the temporal frequency of the swimming gait, but why and how does this happen without affecting the spatial form of the swimming gait? In any case, our analysis of the physical and sensory determinants of the swimming gait provides a framework for continued investigation of such questions within a tractable model system.

We thank M. Chalfie for useful conversations. This work was supported by the Sloan, McKnight and National Science Foundations.

References

- Bargmann, C. I. and Avery, L. (1995). Laser killing of cells in *Caenorhabditis elegans*. *Methods Cell Biol.* **48**, 225-250.
- Berg, H. C. (1993). *Random Walks in Biology*. Princeton, NJ: Princeton University Press.
- Berg, H. C. and Turner, L. (1979). Movement of microorganisms in viscous environments. *Nature* **278**, 349-351.
- Brenner, H. (1961). The slow motion of a sphere through a viscous fluid towards a plane surface. *Chem. Eng. Sci.* **16**, 242-251.
- Brenner, S. (1974). The genetics of *Caenorhabditis elegans*. *Genetics* **77**, 71-94.
- Chalfie, M., Sulston, J. E., White, J. G., Southgate, E., Thomson, J. N. and Brenner, S. (1985). The neural circuit for touch sensitivity in *Caenorhabditis elegans*. *J. Neurosci.* **5**, 956-964.
- Chelur, D. S., Ernstrom, G. G., Goodman, M. B., Yao, C. A., Chen, L., O'Hagan, R. and Chalfie, M. (2002). The mechanosensory protein MEC-6 is a subunit of the *C. elegans* touch-cell degenerin channel. *Nature* **420**, 669-673.
- Chung, S. H., Clark, D. A., Gabel, C. V., Mazur, E. and Samuel, A. D. (2006). The role of the AFD neuron in *C. elegans* thermotaxis analyzed using femtosecond laser ablation. *BMC Neurosci.* **7**, 30.
- Cohen, E., Riesenfeld, R. F. and Elber, G. (2001). *Geometric Modeling with Splines*. Natick, MA: AK Peters.
- Cronin, C. J., Mendel, J. E., Mukhtar, S., Kim, Y. M., Stirbl, R. C., Bruck, J. and Sternberg, P. W. (2005). An automated system for measuring parameters of nematode sinusoidal movement. *BMC Genet.* **6**, 5.
- Driscoll, M. and Chalfie, M. (1991). The mec-4 gene is a member of a family of *Caenorhabditis elegans* genes that can mutate to induce neuronal degeneration. *Nature* **349**, 588-593.
- Duysens, J., Clarac, F. and Cruse, H. (2000). Load-regulating mechanisms in gait and posture: comparative aspects. *Physiol. Rev.* **80**, 83-133.
- Goodman, M. B. and Schwarz, E. M. (2003). Transducing touch in *Caenorhabditis elegans*. *Annu. Rev. Physiol.* **65**, 429-452.
- Gray, J. and Hancock, G. J. (1955). The propulsion of sea urchin sperm. *J. Exp. Biol.* **32**, 802-814.
- Gray, J. and Lissmann, H. W. (1964). The locomotion of nematodes. *J. Exp. Biol.* **41**, 135-154.
- Holwill, M. E. J. and Burge, R. E. (1963). A hydrodynamic study of the motility of flagellated bacteria. *Arch. Biochem. Biophys.* **101**, 249-260.
- Karbowsky, J., Cronin, C. J., Seah, A., Mendel, J. E., Cleary, D. and Sternberg, P. W. (2006). Conservation rules, their breakdown, and optimality in *Caenorhabditis* sinusoidal locomotion. *J. Theor. Biol.* **242**, 652-669.
- Li, W., Feng, Z., Sternberg, P. W. and Xu, X. Z. S. (2006). A *C. elegans* stretch receptor neuron revealed by a mechanosensitive TRP channel homologue. *Nature* **440**, 684-687.
- Niebur, E. and Erdos, P. (1993). Theory of the locomotion of nematodes: control of the somatic motor neurons by interneurons. *Math. Biosci.* **118**, 51-82.
- O'Hagan, R., Chalfie, M. and Goodman, M. B. (2005). The MEC-4 DEG/ENaC channel of *Caenorhabditis elegans* touch receptor neurons transduces mechanical signals. *Nat. Neurosci.* **8**, 43-50.
- Purcell, E. M. (1977). Life at Low Reynolds number. *Am. J. Phys.* **45**, 3-11.
- Sulston, J. and Hodgkin, J. (1988). Methods. In *The Nematode Caenorhabditis elegans* (ed. W. B. Wood), pp. 587-606. Cold Spring Harbor, NY: Cold Spring Harbor Press.
- Syntichaki, P. and Tavernarakis, N. (2004). Genetic models of mechanotransduction: the nematode *Caenorhabditis elegans*. *Physiol. Rev.* **84**, 1097-1153.
- Tavernarakis, N., Shreffler, W., Wang, S. L. and Driscoll, M. (1997). *unc-8*, a DEG/ENaC family member, encodes a subunit of a candidate mechanically gated channel that modulates *C. elegans* locomotion. *Neuron* **18**, 107-119.
- Wallace, H. R. (1959). The movement of eelworms in water films. *Ann. Appl. Biol.* **46**, 74-94.
- White, J. G., Southgate, E., Thomson, J. N. and Brenner, S. (1976). The structure of the ventral nerve cord of *Caenorhabditis elegans*. *Philos. Trans. R. Soc. Lond. B Biol. Sci.* **275**, 327-348.
- White, J. G., Southgate, E., Thomson, J. N. and Brenner, S. (1986). The structure of the nervous system of the nematode *C. elegans*. *Philos. Trans. R. Soc. Lond. B Biol. Sci.* **314**, 1-340.